Modelling and recursive power control of horizontal variable speed wind turbines

H.P Wang*, A. Pintea, N. Christov***, P. Borne****, D. Popescu****

* Nanjing University of Science and Technology, Automation School, China
(Corresponding author: hp.wang@njust.edu.cn)
** University "Politehnica" of Bucharest, Splaiul Independentei, nr. 313, Romania
(andreea.pintea@gmail.com, popescu_upb@yahoo.com)
*** Lille University of Science and Technology, 59651, Villeneuve d'Ascq, France
(nicolai.christov@univ-lille1.fr)
**** Ecole Centrale de Lille, 59651, Villeneuve d'Ascq, France (pierre.borne@ec-lille.fr)

Abstract: The paper deals with the modeling and power control of horizontal variable speed wind turbines using a new recursive controller. The problem considered is to realize a multi-objective control scheme covering the entire wind turbine working domain. The proposed recursive model free controller (RMFC) is designed to realize a compromise between the maximum-power-point trajectory tracking under realistic wind energy exploitation, the desired rotor speed reference trajectory tracking and the need of decreasing the solicitations induced in the mechanical structure of the turbine. The RMFC uses only the turbine output measurement and does not require knowledge of turbine parameters. It has a very simple structure and can be easily implemented in computer control systems. The effectiveness and robustness of the proposed control approach are proven by numerical simulations.

Keywords: wind turbines, power regulation, recursive control algorithms.

1. INTRODUCTION

Wind turbines function in extremely dynamical and unpredictable environmental conditions. The energy production is entirely dependent on the wind therefore an efficient extraction of the energy implies a good knowledge of the wind characteristics. The stochastic nature of the wind and the difficulties encountered by the scientists in conceiving predictions regarding wind's speed, intensity or direction in time, make the energy production be sensitive to any sudden wind burst. The goals for the control of the wind turbines depend on the working regimes and will be briefly defined in the following sections. We have focused our interest on finding the command that would provide the optimum power level with the minimum mechanical stress sensed by the turbine's physical structure within turbulent conditions and as well as in situations of steady winds.

Many control solutions are proposed in the literature, all being conceived for a specific model, simplified or sophisticated, linear or nonlinear. In general, the existing control methods are based on the use of linear models supposed to closely approximate the nonlinear turbine dynamics (Lescher et al. 2006; Yao et al. 2009; Li et al. 2008; Hand 1999). Linear models allow obtaining relatively simple and analytical solutions (LQR, poles placement (Nourdine et al. 2010; Munteanu et al. 2008; Bianchi et al. 2007)), which are easily implementable in practical applications. However, the linear models bring the disadvantage that the controller's performances are guaranteed only for the particular operating point specified in the linearization phase.

On the other hand, the nonlinear model based methods can ensure larger operating regimes (Kebairi et al. 2009; Boukhezzar and Siguerdidjane 2010) but their performances are strongly dependent on the availability of an accurate turbine model. In (Hand 1999) a comparative analysis of a PID controller designed for both linear and nonlinear models of a wind turbine is presented. In both cases, though, the controller is highly dependent on the model parameters. In this paper, we propose to utilize a Recursive Model Free Controller (RMFC) (Wang et al. 2010a; Wang 2011) for horizontal variable speed wind turbine systems. The particularity of our controller is that it only uses the system output measurements and it does not require knowledge of the turbine parameters. Its structure is recursive, proportional (P) but with a time varying gain and it can be easily implemented in computer control systems. We shall demonstrate the performances of this controller for the wind turbine whose nonlinear model is briefly detailed in Section 2 of the paper. In Sections 3 and 4 the control objectives are formulated and a RMFC for a wind turbine system is developed. The controller performances are analyzed in Section 5, and at the end in Section 6, some concluding remarks are given.

2. WIND TURBINE SYSTEM DESCRIPTION AND MODELING

2.1 Wind turbine system description

We start by presenting the wind turbine system (WTS) modeling procedure. To easily obtain the wind turbine model, we have split the general WTS into several interconnected subsystems: aerodynamic, mechanical, electrical and pitch

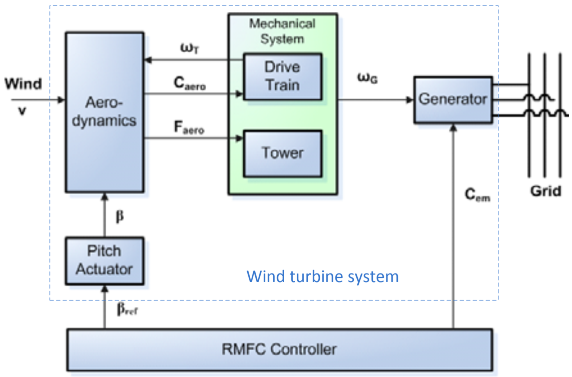

Fig. 1. WTS and its corresponding control scheme.

actuator. Figure 1 contains the above mentioned four blocks and the recursive controller connected to the turbine. We will offer a short description for each of the four blocks that define the WTS. The aerodynamic subsystem is mainly defined by the turbine's rotor. Its dynamics are modeled through analytical expressions of the forces that appear when the wind interacts with the rotor blades.

The mechanical subsystem includes the tower and the drive train. The latter transmits the rotation of the turbine rotor to the electrical generator. Its structure depends on the wind turbine technology. For the WTS considered in this paper the drive train uses the direct drive transmission technique which can be modelled as two rigid bodies linked by a flexible shaft as shown in Fig. 2a (Bianchi et al. 2007). The generator subsystem contains both the generator and all electrical devices that realize the connection of the turbine to the electrical grid or directly to consumer devices.

The pitch actuator ensures the regulation on the above rated wind speed through collective rotation of the blades. We have made a simplifying hypothesis and we have considered that all blades turn simultaneously with the same pitch angle in the same direction. Blade pitch regulation offers means for varying the rotational speed in order to extract more power at different wind speeds and also to regulate the extracted power at the desired level.

2.2 Mathematical modeling procedure

A mechanical system of arbitrary complexity can be described by the following equation (Bianchi et al. 2007).

$$M \cdot \ddot{q} + C_d \cdot \dot{q} + K \cdot q = Q(\dot{q}, q, t, u) \qquad (4)$$

where M is the mass matrix, C_d is the damping matrix and K is the stiffness matrix respectively. Q is the vector of the forces that act on the system, while q is the generalized

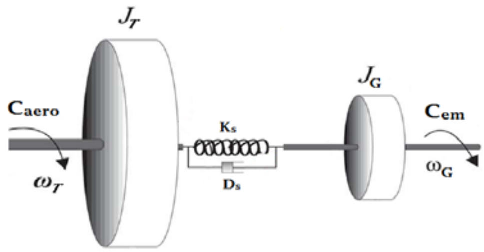

Fig. 2. a) Direct shaft transmission system (two-mass model).

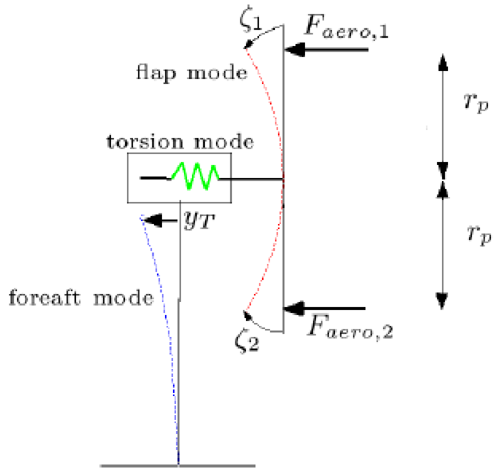

Fig. 2. b) The mechanical structure of the WTS.

coordinate vector. Q depends on q, the derivative of q, time and the control signal u. We will apply this equation on our mechanical structure, represented as in Fig. 2.b.

In order to do so, we have defined q as

$$q = (\omega_T, \omega_G, \zeta, y_T)^T \qquad (5)$$

where ω_T is the angular speed of the turbine rotor, ω_G stands for the angular speed of the generator (Fig. 1), and ζ and y_T represent the bending movement of the blades under the wind pressure and the horizontal displacement of the tower respectively (Fig. 2). We have considered that the forces exerted on both blades are identical, therefore $F_{aero1} = F_{aero2} = F_{aero}$ leads to $\zeta_1 = \zeta_2 = \zeta$. Similarly, the vector of the generalized forces is

$$Q = (C_{aero}, -C_{em}, F_{aero}, 2 \cdot F_{aero})^T \qquad (6)$$

with C_{aero} the aerodynamic torque, C_{em} the electromagnetic torque and F_{aero} the thrust force, which acts on the rotor and is considered applied on a point situated at the distance r_P on each blade from the hub of the rotor.

The determination of the models of the four subsystems described in Section 2.1 is based on the Lagrange equation

$$\frac{d}{dt}\left(\frac{\delta E_c}{\delta \dot{q}_i}\right) - \frac{\delta E_c}{\delta q_i} + \frac{\delta E_d}{\delta \dot{q}_i} + \frac{\delta E_P}{\delta q_i} = Q \qquad (7)$$

where E_c, E_d, and E_p denote the kinetic, dissipated and potential energies of the mechanical structure represented in Fig. 2, and q_i and $\dot{q}_i$ are the elements of the generalized coordinate vector (5) and their derivatives, respectively. Q used in (7) is the same as the one defined in (4) and it is equal to (6). The reader must see equation (6) as a matrix representation of (4); therefore the equations that derive from (6) can be grouped to provide (4).

The kinetic energy is defined as

$$E_c = \frac{J_T}{2}\cdot\omega_T^2 + \frac{J_G}{2}\cdot\omega_G^2 + \frac{M_T}{2}\cdot\dot{y}_T^2 + M_P\cdot(\dot{y}_T + r_P\cdot\dot{\zeta})^2 \tag{8}$$

with J_T and J_G the turbine rotor and generator moments of inertia, M_T encapsulates the tower and nacelle mass, and M_P is the blade mass. In turn, the potential energy can be written as

$$E_P = \frac{k_A}{2}\cdot{\theta_S}^2 + k_P\cdot(r_P\cdot\zeta)^2 + \frac{k_T}{2}\cdot y_T^2 \tag{9}$$

where k_A, k_P and k_T are the spring coefficients of the drive shaft, blades and tower, and $\theta_S=\theta_T-\theta_G$ is the thrust of the driving shaft, with θ_T and θ_G the angular positions of the rotor and generator axis. Note that θ_S should be maintained as close to zero as possible. Similarly, the dissipation energy is

$$E_D = \frac{d_A}{2}\cdot{\dot{\theta}_S}^2 + d_P\cdot(r_P\cdot\dot{\zeta})^2 + \frac{d_T}{2}\cdot\dot{y}_T^2 \tag{10}$$

with d_A, d_P and d_T the damping coefficients of the blade, drive shaft and tower and $\dot{\theta}_S = \omega_S = \omega_T - \omega_G$.

2.2.1 Aerodynamic subsystem model

The wind that intercepts the rotor creates an aerodynamic thrust force F_{aero} and an aerodynamic torque C_{aero}. The result of the torque action is the rotational motion of the turbine. The C_{aero} and F_{aero} act on the rotor are expressed in terms of non-dimensional power and thrust coefficients C_P and C_T as (Bianchi et al. 2007)

$$C_{aero} = \frac{1}{2}\cdot\rho\cdot\pi\cdot R^2\cdot C_P(\lambda,\beta)\cdot\frac{v^3}{\omega_T} \tag{11}$$

$$F_{aero} = \frac{1}{2}\cdot\rho\cdot\pi\cdot R^2\cdot C_T(\lambda,\beta)\cdot v^2 \tag{12}$$

where ρ is the air density, R is the blade radius, and v is the average speed of the wind. Note that the power and thrust coefficients C_P and C_T are unique for each turbine and depend on two parameters λ and β, where λ is the tip speed ratio defined as $\lambda = \frac{\omega_T\cdot R}{v}$ (the ratio between the peripheral blade speed and the speed of the wind), and β is the pitch angle of the blades.

The power coefficient C_P is defined as

$$C_p(\lambda,\beta) = \frac{P_{extracted\_from\_the\_wind}}{P_{available\_in\_the\_wind}}. \tag{13}$$

C_P is inferior to 1. According to A. Betz, no turbine can capture more than 59.3% of the kinetic energy in the wind (Hau 2006; Burton et al. 2002; Munteanu et al. 2008). Various expressions for the power coefficient exist, such as exponential expressions in (Ramakrishnan and Srivatsa 2008; Papathanassiou and Papadopoulos 1994), or a sinusoidal expression in (Winkelman and David 1983). In this paper, the power coefficient is defined as

$$C_p(\lambda,\beta) = 0.5176\cdot\left(\frac{116}{\lambda_i} - 0.4\cdot\beta - 5\right)\cdot e^{\frac{-21}{\lambda_i}} + 0.0068\cdot\lambda, \tag{14}$$

$$\frac{1}{\lambda_i} = \frac{1}{\lambda + 0.08\cdot\beta} - \frac{0.035}{\beta^3+1} \tag{15}$$

and the thrust coefficient is computed as

$$\begin{aligned} C_T(\lambda,\beta) &= (0.000018851\cdot\beta + 0.000077364)\cdot\lambda^3 \\ &+(-0.00082131\cdot\beta - 0.0052121)\cdot\lambda^2 + \\ &(-0.0024011\cdot\beta + 0.1595)\cdot\lambda + 0.12105\cdot\beta - 0.25697 \end{aligned} \tag{16}$$

The variations of the power and thrust coefficients with respect to the tip speed ratio and the pitch angle are depicted in the Fig. 3 and Fig. 4, respectively. From (7) the following equation describing the rotor dynamics is obtained (Bianchi et al. 2007; Lescher et al. 2005):

$$J_T\cdot\dot{\omega}_T + d_A\cdot\dot{\theta}_S + k_A\cdot\theta_S = C_{aero}. \tag{17}$$

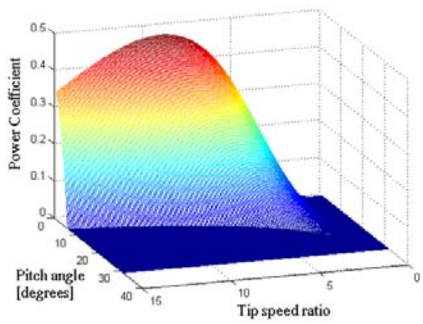

Fig. 3. Power coefficient variation with respect to λ and β.

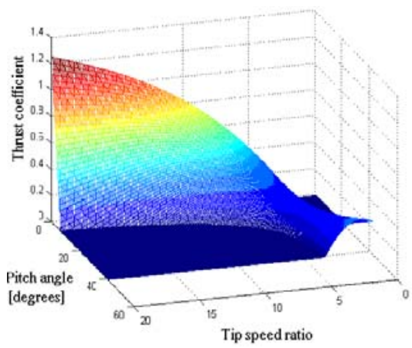

Fig. 4. Thrust coefficient variation with respect to λ and β.

2.2.2 Mechanical subsystem model

In this paper we have taken into account three main oscillating modes that are affecting the mechanical structure of the turbine see Fig. 5. The considered oscillating modes

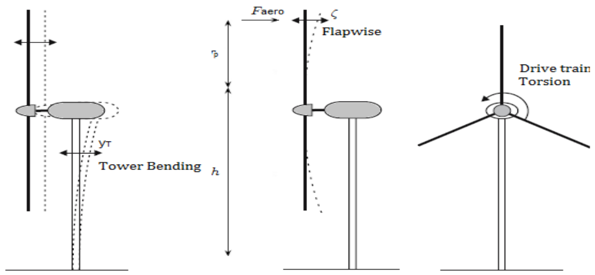

Fig. 5. WTS mechanical part oscillating modes.

are the horizontal bending movement of the tower, the first oscillating mode of the blades and the thrust of the drive train (Wright 2004; Lescher 2005). The equations describing the tower and blades movements under the action of the wind are obtained from (7) (Bianchi et al. 2007; Lescher et al. 2005) and are given below:

$$2 \cdot M_P \cdot (\ddot{y}_T + r_P \cdot \ddot{\zeta}) + 2 \cdot d_P \cdot r_P \cdot \dot{\zeta} + 2 \cdot k_P \cdot r_P \cdot \zeta = F_{aero} \quad (18)$$

for the blades, and

$$(M_T + 2 \cdot M_P) \cdot \ddot{y}_T + 2 \cdot M_P \cdot r_P \cdot \ddot{\zeta} + d_T \cdot \dot{y}_T + k_T \cdot y_T = 2 \cdot F_{aero} \quad (19)$$

for the tower, where M_P and M_T are respectively the blade mass and the tower and nacelle mass.

2.2.3. Generator subsystem model

In order to simplify the model, the generator dynamics were not modelled in detail, the only variable of interest being the torque that the generator develops while producing electrical energy. Thus we have included into our model the equation modeling the generator axis movement, also derived from (7):

$$J_G \cdot \dot{\omega}_G - d_A \cdot \dot{\theta}_S - k_A \cdot \theta_S = -C_{em} \,. \quad (20)$$

2.2.4 The pitch actuator model

The pitch actuator is described by (Lescher 2005)

$$T_\beta \dot{\beta} + \beta = \beta_{ref} \quad (21)$$

where T_β is the time constant, β is the actual pitch angle of the blades and β_{ref} is the desired pitch angle. To prevent damaging the pitch servomotor, it is imposed that the pitch angle shall not exceed *45°* in both rotating directions and also that the servomotor speed will not surpass *10 °/s*. Thus, in the simulation studies in Section 5, equation (21) is completed with two saturation blocks for the angular position and angular speed, respectively (see Fig. 6).

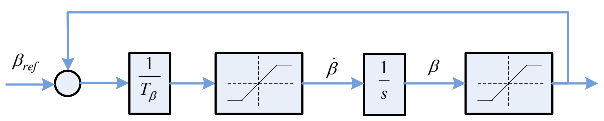

Fig. 6. Pitch servomotor subsystem.

2.2.5 The wind model

The wind speed is modeled as a sum of two-components (Nichita et al. 2002):

$$v(t) = v_m(t) + v_t(t) \quad (22)$$

where $v_m(t)$ denotes the low-frequency long term fluctuations component and $v_t(t)$ represents the turbulent, rapidly varying component. According to (Lescher et al. 2006; Jianlin et al 2008; Munteanu et al. 2008), $v_t(t)$ is described by

$$\dot{v}_t(t) = -\frac{1}{T_v} \cdot v_t + n(t) \quad (23)$$

where $n(t)$ is a zero-mean Gaussian white noise and T_v is a time constant depending on the stochastic properties of the wind. With respect to the turbulent component, v_m can be considered as constant and it is representing the average value of the wind speed.

2.3. Wind turbine model

Assuming that the angular position and speed limitations are respected, from equations (17)-(23) one obtains the following WTS state space representation

$$\dot{x}(t) = f(x,t) + g(x,u,t) + h(t) \quad (24)$$

$$y(t) = \varphi(x,u) \quad (25)$$

with:

$$f(x,t) = \begin{pmatrix} \theta_s \\ \dot{\zeta} \\ \dot{y}_T \\ \frac{-d_A}{J_T} \cdot \dot{\theta}_s - \frac{k_A}{J_T} \cdot \theta_s \\ \frac{-d_A}{J_G} \cdot \dot{\theta}_s + \frac{k_A}{J_G} \cdot \theta_s \\ -d_P \cdot M_f \cdot \dot{\zeta} - k_P \cdot M_f + \frac{d_T}{r_P \cdot M_T} \cdot \dot{y}_T + \frac{k_T}{r_P \cdot M_T} \cdot y_T \\ \frac{2 \cdot r_p \cdot d_p}{M_T} \cdot \dot{\zeta} + \frac{2 \cdot k_p \cdot r_p}{M_T} \cdot \zeta - \frac{d_T}{M_T} \cdot \dot{y}_T - \frac{k_T}{M_T} \cdot y_T \\ -\frac{1}{T_\beta} \\ -\frac{1}{T_v} \cdot v \end{pmatrix}, \quad g(x,u,t) = \begin{pmatrix} 0 \\ 0 \\ 0 \\ \frac{1}{J_T} \cdot c_1 \cdot v^2 \cdot C_P(\lambda,\beta) \\ \frac{-C_{em}}{J_G} \\ \frac{(M_T - 2M_P)}{2 \cdot M_P \cdot M_T \cdot r_p} \cdot c_1 \cdot v^2 \cdot C_T(\lambda,\beta) \\ \frac{1}{M_T} \cdot c_1 \cdot v^2 \cdot C_T(\lambda,\beta) \\ \frac{1}{T_\beta} \cdot \beta_{ref} \\ \frac{1}{T_v} \cdot v_m \end{pmatrix}$$

$h(t) = \left[0,0,0,0,0,0,0,0,n(t)\right]^T$, $\varphi(x,u) = (\omega_T, \omega_G C_{em}, \zeta, y_T)^T$.

Here $x(t) = (\theta_s, \zeta, y_T, \omega_T, \omega_G, \dot{\zeta}, \dot{y}_T, \beta, v)^T$, $u(t) = (\beta_{ref}, C_{em})^T$ and $y(t) = (\omega_T, P_{el}, \zeta, y_T)^T$ are the turbine state, control and output vectors, respectively, $M_f = (M_T + 2M_P)/(M_P \cdot M_T)$, $c_1 = \rho \pi R^2 / 2$ and P_{el} is the generated electrical power.

Because of the nonlinearities of C_{aero} and F_{aero}, the obtained WTS model (24-25) is highly nonlinear and complex.

3. WORKING REGIMES AND CONTROL OBJECTIVES

In practice, based on the average value of the wind speed, the functioning domain of the wind turbines can be divided into two main operation regions of power optimisation and power limitation, as illustrated in Fig. 7. Each region has its own

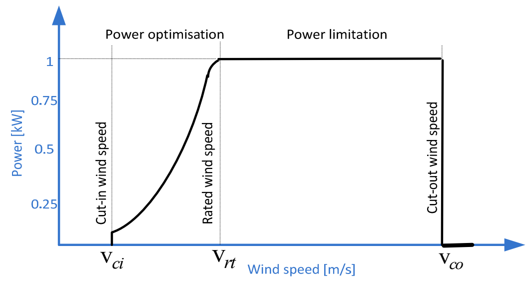

Fig.7. WTS power curve with respect to wind speed.

particularities which require the controller objectives to be defined separately.

The first region describes the wind turbine operation during weak winds. It is characterized by wind speeds comprised between v_{ci}, the *cut-in wind speed* (normally its value varies around 4 m/s), and v_{rt} , *the rated wind speed* (which is chosen usually around 13 m/s) (Zhang et al. 2008). Within this interval, the extracted power is lower than the rated output power of the turbine generator (Jelavic et al. 2006). In consequence, the task of the control system is to maximize the power extraction. The pitch angle of the blades is fixed to an optimum value which is normally close to 0º. This ensures that the blades have the maximum incidence with the wind streams. In the same time, the electric torque is controlled so that the turbine can operate at optimum tip speed ratio denoted as λ_{opt}. By referring to Fig. 3, one can observe that a wind turbine cannot optimally operate at all the speeds of the wind. Therefore, the control algorithm computes the maximum value of the power coefficient, denoted as $C_{P,opt}$ which corresponds to optimum values of the tip speed ratio λ_{opt} and the pitch angle of the blades β_{opt} respectively. Then the generator optimal power is calculated as (Beltran et al. 2008).

$$P_{opt} = C_{em,opt} \cdot \omega_{opt} \tag{26}$$

where $C_{em,opt} = \rho \cdot \pi \cdot R^3 \cdot C_{P,\max}(\lambda_{opt}, \beta_{opt}) \cdot v^2 / 2\lambda_{opt}$ and $\omega_{opt} = \lambda_{opt} \cdot v / R$ are the generator optimal torque and speed respectively. Hence in this region, the controller has the objective of ensuring that the turbine tip speed ratio follows as close as possible the optimum value λ_{opt} for β_{opt}. This results in a power coefficient C_P that closes to $C_{P,opt}$ and ensures that the extracted power is maximal. The second operation region defines the functioning of the wind turbine during powerful winds with speeds that vary between v_{rt} (13 m/s) and v_{co}, *the cut-out wind speed* (25m/s) (Zhang et al. 2008). Noted that in the regions where wind speeds are inferior to v_{ci} or superior to v_{co}, the wind turbine is shut-down for economical and security reasons. The power that can be extracted:

$$P_a = \rho_{air} \cdot \pi \cdot R^2 \cdot C_p(\lambda, \beta) \cdot v^3 / 2$$

surpasses the rated output power P_n and its limitation is therefore needed.

Besides the need of power regulation, a minimization of the mechanical solicitations induced in the mechanical structure of the turbine (ζ and y_T) is also imposed. Considering the power curve (Fig. 7), the WTS control objectives can be formulated in the following way:

1) Regarding the operating regimes: we want that the electrical power extracted to optimally track the electrical power reference $P_{el,ref}$ which is defined as

$$P_{el,ref} = \begin{cases} P_{opt}, & v_{ci} \le v \le v_{rt} \\ P_n, & v_{rt} \le v \le v_{co} \end{cases} \tag{27}$$

2) Concerning the regulation purpose: we want a good tracking of the rotor speed reference $\omega_{T,ref}$ defined as

$$\omega_{T,ref} = \omega_{T,n}, \quad v_{ci} \le v \le v_{co} \tag{28}$$

where $\omega_{T,n}$ is the nominal angular speed of the rotor.

3) Also we want to ensure the minimization of the mechanical solicitations ζ and y_T. Their desired values are defined as ζ_{ref} and $y_{T,ref}$ and they should be as close to zero as possible in the working regime $v_{ci} \le v \le v_{co}$.

4. RECURSIVE MODEL FREE CONTROLLER

As stated before, in order to achieve the above mentioned WTS control objectives we shall use a Recursive Model Free Controller (RMFC) (Wang et al. 2010a). In this section we briefly describe the RMFC design and its use for the WTS control.

The RMFC is a generalization of the so-called Derived Piecewise Continuous Controller (DPCC) proposed in (Wang et al. 2010a; Wang et al. 2010c). Both DPCC and RMFC were developed using the theory of a particular class of hybrid systems called piecewise continuous systems (Koncar and Vasseur 2003; Wang et al. 2010b; Wang 2011). We refer to (Wang et al. 2010a) as the main reference for RMFC design and performance analysis.

In the case of WTS, the following RMFC representation can be used:

$$\lambda_c(t) = |e(t)| \cdot (c_o(t) - y(t)) + \xi(t) \cdot \lambda_c(t) \tag{29}$$

$$u(t) = \gamma \cdot \lambda_c(t) \tag{30}$$

where $\lambda_c(t) \in \Re^4$ is the controller state vector with the same dimension as the WTS output, $e(t) = c_o(t) - y(t) \in \Re^4$ is the output tracking error, $\xi(t) \in \Re$ is the controller tracking coefficient, $\gamma \in \Re^{2\times 4}$ is the controller output matrix,

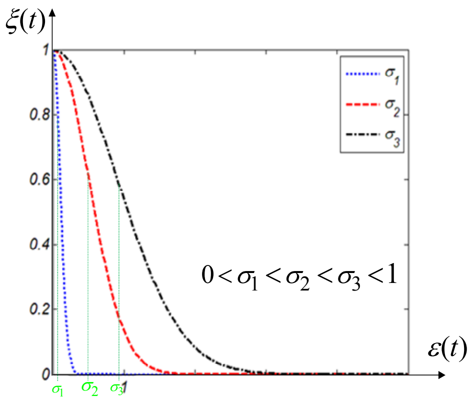

Fig. 8. Evolution of the tracking coefficient $\xi(t)$ as a function of the tracking error *ε(t)* for different σ .

$u(t) \in \Re^2$ is the controller output and

$$c_o(t) = (\omega_{T,ref}, P_{el,ref}, \zeta_{ref}, y_{T,ref})^T \quad (31)$$

is the desired output reference vector.

In order to obtain $e(t) \to 0$, the tracking coefficient $\xi(t)$ is tuned as

$$\xi(t) = \exp(-\varepsilon^2(t)/(2\cdot\sigma^2)) \quad (32)$$

with $\varepsilon(t) = \sqrt{e^T(t)\cdot e(t)}$ and $0 < \sigma \le 1$. It follows from (32) that $0 < \xi(t) \le 1$ and having $\xi \to 1$ for $\varepsilon(t) \to 0$, $\xi \to 0$ for $\varepsilon(t) \to \infty$.

The first and second derivatives of $\xi(t)$ are

$$\frac{\partial \xi(t)}{\partial \varepsilon} = -\frac{\varepsilon(t)}{\sigma^2}\cdot\xi(t) \le 0, \quad \text{for } \varepsilon(t) \ge 0 \quad (33)$$

$$\frac{\partial^2 \xi(t)}{\partial \varepsilon^2} = -\frac{1}{\sigma^2}\cdot\left[1 - \frac{\varepsilon^2(t)}{\sigma^2}\right]\cdot\xi(t) \quad (34)$$

which means that the tracking coefficient $\xi(t)$ decays exponentially with a variable speed and its evolution depends on the value of $1-(\varepsilon^2(t)/\sigma^2)$ (Wang et al. 2010c). Fig. 8 illustrates the evolution of $\xi(t)$ as a function of $\varepsilon(t)$ for $0 < \sigma_1 < \sigma_2 < \sigma_3 < 1$. It can be seen that by varying σ , the tracking coefficient decay speed can be modified, allowing to affect thus the controller performances. It follows from (29) and (30) that

$$u(t) = \gamma\cdot\lambda_c(t) = k(t)\cdot e(t) \quad (35)$$

with $k(t) = \gamma\cdot\varepsilon^2(t)/(1-\xi(t))$. Using the first order approximation of the exponential term in (32), one obtains

$$\xi(t) = \exp(-\varepsilon^2(t)/(2\cdot\sigma^2)) \approx 1-(\varepsilon^2(t)/(2\cdot\sigma^2)) . \quad (36)$$

By taking into account (35), *k*(*t*) can be calculated as

$$k(t) = \gamma\cdot\varepsilon^2(t)/(1-\xi(t)) \approx 2\cdot\gamma\cdot\sigma^2/\varepsilon(t) \quad (37)$$

and thus the proposed recursive controller is given by

$$u(t) \approx ((2\cdot\gamma\cdot\sigma^2)/\varepsilon(t))\cdot e(t) . \quad (38)$$

In (35) only σ and γ are the configurable parameters. The command, as it can be seen in (35) is proportional to the output tracking error $e(t)$, through a proportional term. It can be seen that RMFC has a classical proportional controller structure with a time varying auto-adjusted proportional gain whose value depends on the tracking error $e(t)$. Thus RMFC can be easily implemented in computer control systems. Bellow we will detail the simulation conditions and the obtained results. Note that the simulations are done for the nonlinear WTS model (22). This highlights the fact that RMFC makes possible to obtain good performances for the entire WTS functioning domain.

5. SIMULATION RESULTS

The performances of the proposed controller are studied by numerical simulations done with Matlab/Simulink for the nonlinear WT model (24-25) taking into account the pitch angular position and speed limitations described in Section 2.2.4. For the wind model described in Section 2.2.5, the long term fluctuation component $v_m(t)$ is considered as a sum of a constant term of 13 m/s and a low-frequency sinusoidal function. The turbulent component $v_t(t)$ is determined using (22) with T_v = 2 s and white noise variance of 3.57. In this way the resulting wind speed *v(t)* varies between 5 m/s and 18 m/s, and consequently covers the entire WT functioning regime (see Fig. 9).

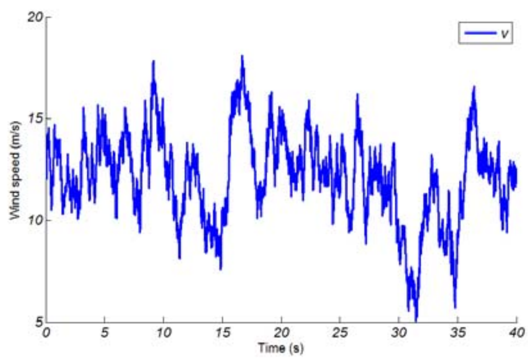

Fig. 9. Wind speed *v(t)*.

The parameters of the WTS are listed in Table I. The two configurable parameters of the RMFC are

$$\gamma = \begin{bmatrix} 1 & 0 & 0 & 0 \\ 0 & 1 & 0 & 0 \end{bmatrix}, \sigma = 0.05.$$

The simulations done have proven that the regulation goals are met. The WTS output responses and control signals are illustrated in Fig. 10 - Fig. 13 and Fig. 14 - Fig. 15, respectively. For the first functioning regime, the maximization of the output power was calculated with respect to a reference of $P_{el,ref} = 4\times10^5$ W. The RMFC ensures not only the power and rotor speed reference tracking but also makes possible to significantly decrease the solicitations induced in the mechanical structure of the turbine. The blades and the tower have deviations of about *3* mm and *2* cm, respectively; therefore they can be seen as insignificant compared to the blade length of *17* m and the tower height of around *50* m. The shaft angular position and speed variations values decay to zero as illustrated in Fig. 15, and demonstrate the effectiveness of the proposed WTS control.

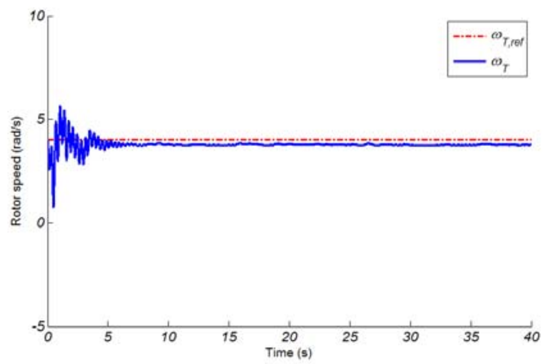

Fig. 10. Turbine rotor angular speed with its reference.

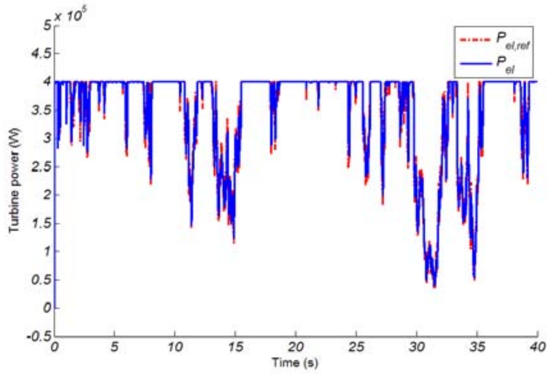

Fig. 11. Electrical power output with its reference.

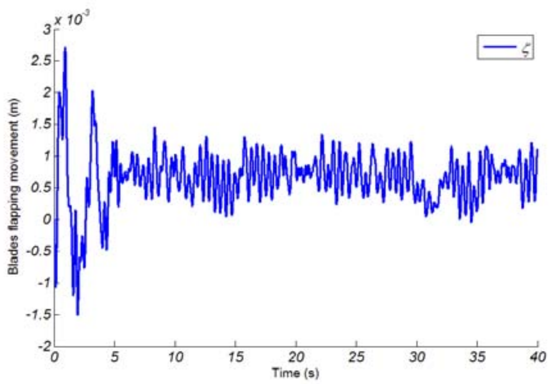

Fig. 12. Blades flapping movements.

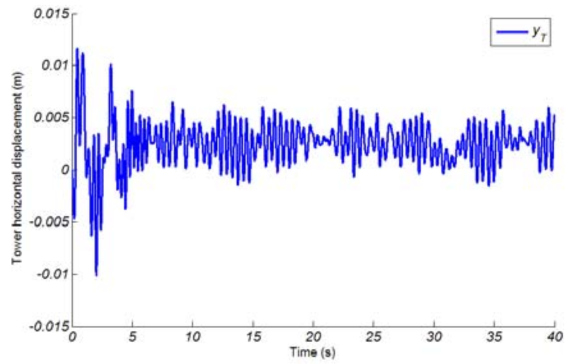

Fig. 13. Tower horizontal displacements.

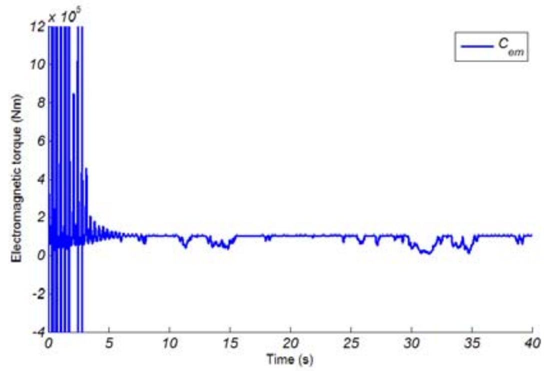

Fig.14. Electromagnetic torque input signal.

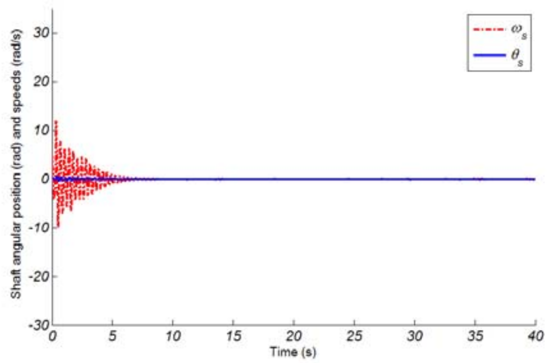

Fig.15. Shaft angular position and speed variations.

6. CONCLUSIONS

This paper presents new nonlinear modeling and power control approaches for horizontal variable speed wind turbines. The proposed recursive controller makes possible to achieve a trade-off between the maximization of the power extraction, the desired rotor speed reference tracking, and the need of decreasing the solicitations induced in the mechanical structure of the turbine. This controller has a very simple structure, does not require knowledge of turbine parameters and can be easily implemented and used for the entire functioning regime of the turbine.

Table 1. Wind turbine numerical values

Symbol	Physical measure	Value
J_T	Turbine inertia	214 000 Kg * m^2
J_G	Generator inertia	41 Kg * m^2
M_T	Tower and nacelle mass	35000 kg
M_p	Blade mass	3000 kg
k_P	Blade Stiffness Coefficient	1000 Kg* m^2/s^2
k_T	Tower Stiffness Coefficient	8500 Kg* m/s^2
k_A	Drive Shaft Stiffness Coefficient	11000 Kg* m^2/s^2
d_P	Blade Damping coefficient	10 000 Kg* m^2/s
d_T	Tower Damping coefficient	50 000 Kg* m/s
d_A	Drive shaft damping coefficient	60 000 Kg* m^2/s
r_P	Distance from the rotor hub	8 m
N	Number of blades	2
D	The rotor diameter	34 m
P_n	Nominal Power	400 kW
$C_{em,nom}$	Nominal Generator Torque	100000Nm
$\omega_{T,n}$	Nominal angular speed of the rotor	4 rad/s
T_β	Time constant of the pitch actuator	0.18 s

REFERENCES

Beltran, B., Ahmed-Ali, T., and El Hachemi Benbouzid, M. (2008). *Sliding mode power control of variable-speed wind energy conversion systems*, IEEE Tran. Energy Conversion, Vol. 23, No. 2, pp. 551-558.

Bianchi, D. F., Battista, H., and Mantz, R., J. (2007). *Wind turbine control systems, principles, modeling and gain scheduling design*, Springer-Verlag, London.

Boukhezzar, B. and Siguerdidjane, H. (2010). *Comparison between linear and nonlinear control strategies for variable speed wind turbine power capture optimization*, in Proc. 4th Int. Conf. and Exhibition on Ecologic Vehicles Renewable Energies, Monaco, March 26-29, Control engineering practice, vol. 18, no. 12, pp 1357-1368.

Burton, T., Sharpe, D., Jenkins, N., and Bossanyi, E. (2002). *Wind energy handbook*, Wiley&Sons.

Cutululis, N., A., Munteanu, and I., Ceanga, E. (2002). *Optimal control structure for variable speed wind power system*, The Annals of "Dunarea de Jos" University of Galati, Fascicle III, pp.95-102.

Hand, M., M. (1999). *Variable-speed wind turbine controller systematic design methodology: A comparison of non-linear and linear model based designs*, NREL Technical Report, NREL/TP-500-25540.

Hau, E. (2006). *Wind turbines, Fundamentals, Technologies, Application, Economics*, 2nd Edition, Springer-Verlag, pp. 103.

Jelavic, M., Peric, N., and Petrovic, I. (2006). *Identification of wind turbine model for controller design*, Proc. 12th Int. Power Electronics and Motion Control Conference, EPE-PEMC.

Jianlin, L., Hongyan, X., and Lei, Z. (2008). *Disturbance accommodating LQR method based pitch control strategy for wind turbines*, Proc. Second Int. Symposium on Intelligent Information Technology Application, Shanghai, 21-22 December, pp. 766-771.

Kebairi, A., Bosche, J., and El Hajjaji, A. (2009). *Commande non linéaire d'une grande éolienne*, Proc. Int. Renewable Energy Congress, November 5-7, Tunisia, pp. 160-165.

Lescher, F. and Borne, P. (2005). *Robust gain scheduling controller for pitch regulated variable speed wind turbine*, Studies in Informatics and Control, Vol. 14, No. 4, pp. 299-315.

Lescher, F., Camblong, H., Briand, R., and Curea, R. O. (2006). *Alleviation of wind turbine loads with a LQG controller associated to intelligent micro sensors*, Proc. IEEE Int. Conf. Industrial Technology, Mumbai, pp. 654-660.

Li, J., Xu H., Zhang, L., Zhu, Y., and Hu, S. (2008). *Disturbance accommodation LQR method based pitch control strategy for wind turbines*, Proc. Second Int. Symposium on Intelligent Information Technology Application, Shanghai, pp. 766-771.

Munteanu, I., Bratcu, A., I., Cutululis, N., A., and Ceanga, E. (2008). *Optimal control of wind energy systems – Towards a global approach*, Springer-Verlag.

Nichita, C., Luca, D., Dakyo, B., Ceanga, E., and Cutululis, N., A. (2000). *Modelling non stationary wind speed for renewable energy systems control*, The annals of "*Dunarea de Jos*" University of Galati, Fascicle 3, pp. 29-34.

Nichita, C., Luca, D., Dakyo, B., and Ceanga, E. (2002). *Large band simulation of the wind speed for real time wind turbine simulators*, IEEE Trans. Energy Conversion, Vol. 4, pp. 523-529.

Nourdine, S., Camblong H., Vechiu, I., and Tapia, G. (2010). *Comparison of wind turbine LQG controllers using individual pitch control to alleviate fatigue loads*, Proc. Mediterranean Conf. Control and Automation, Marrakech, Morocco, June 23-25, pp.1591-1596.

Papathanassiou, S. A. and Papadopoulos, M., P. (1994). *Simulation and control of a variable speed wind turbine equipped with a double output induction generator*, Proc. PEMC'94, Warsaw, Poland.

Ramakrishnan, V., and Srivatsa S. K. (2008). *Pitch control of wind turbine generator by using new mechanism*, Journal Electrical Systems, pp.1-15.

Wang, H. P., Vasseur, C., Koncar, and V., Christov, N. (2010a). *Recursive model free controller for trajectory tracking of MIMO nonlinear systems*, Proc. 18th Mediterranean Conference on Control and Automation, Marrakech, Morroco, pp. 431-436.

Wang, H. P., Vasseur, C., Koncar, V., and Christov, N. (2010b). *Design and implementation of robust hybrid control of vision based underactuated mechanical nonminimum phase systems*, Studies in Informatics and Control, Vol. 19, No. 1, pp. 35-44.

Wang, H. P., Vasseur, C., Chamroo, A., Koncar, V., and Christov, N. (2010c). *Modelling and trajectory tracking control of a 2-DOF vision based inverted pendulum*. Control Engineering and applied informatics, Vol. 12, No. 3, pp. 59-66.

Wang, H., P. (2011), *Observation et commande par systèmes a fonctionnement par morceaux: Applications aux* *asservissements visuels*, Saarbrucken : Editions Universitaires Européennes, ISBN 978-631-1-56931-1.

Winkelman, J. R. and David, S., H. (1983). *Control design and performance analysis of a 6MW wind turbine generator.* IEEE Trans. PAS, Vol. 102, No. 5, pp. 1340-1347.

Wright, A. D. (2004). *Modern control design for flexible wind turbines – Technical report*, NREL/TP-500-35816, pp. 23-26.

Yao, X., Gou, C., Xing, Z., Li, Y., Liu S., and Wang, X. (2009). *Pitch regulated LQG controller design for variable speed wind turbine*, Proc. IEEE Int. Conf. on Mechatronics and Automation, Changchun, China, pp.845-849.Zhang, J., Cheng, M., Chen, Z., Fu, X., (2008), *Pitch angle control for variable speed wind turbine*, The Third Conference on Electric Utility Deregulation and Restructuring and Power Technologies, Nanjing, China.